

# CONTROL OF DYNAMIC VOLTAGE RESTORER UNDER VOLTAGE SAG AND NONLINEAR LOAD

Nguyen Trong Huan\*, Ho Nhut Minh\*, Van Tan Luong†

\* Học Viện Công Nghệ Bưu Chính Viễn Thông Cơ Sở Thành Phố Hồ Chí Minh

† Trường Đại học Công nghiệp Thực phẩm Thành Phố Hồ Chí Minh

**Abstract** - In this paper, a nonlinear control scheme for dynamic voltage restorer (DVR) is proposed to reduce the voltage disturbances for loads under grid voltage sags and nonlinear loads. First, the nonlinear model of the system consisting of LC filter is obtained in the dq0 synchronous reference frame. Then, the controller design is performed by using the sliding mode control, where the load voltages are kept almost sinusoidal by controlling the dq0 axis components of the DVR output voltages. With this scheme, the power quality is significantly improved, compared with the conventional proportional-integral (PI) controller under grid voltage sags and nonlinear loads. Simulation studies are performed to verify the validity of the proposed method.

**Keywords** - Dynamic voltage restorer, nonlinear load, sliding mode control, voltage sags.

## I. INTRODUCTION

In recent years, as the penetration of the renewable energy systems into the grid at the point of common coupling (PCC) increases rapidly, the issues of the power quality are paid much attention. The critical power quality issues in distribution systems are related to grid voltage disturbances. Since the application of power electronics devices has been increased in industrial processes, disturbances of the power supply affect the industrial loads. This can cause malfunctions, tripping, or even faults of the load system. The voltage sags, swells, harmonics, unbalances, and flickers, known as power quality issues, are generally considered as critical phenomena of voltage disturbances in distribution systems, in which the voltage sags is a main reason of short-circuit faults [1]-[4].

Several methods have been used to improve the power quality in the distribution networks. A dynamic voltage restorer (DVR) system is one of the best solutions which keep the load voltage at its rated value when the grid voltage drops occur suddenly. The DVR system is composed of a voltage-source inverter (VSI), output LC filters, and an isolated transformer connected between the source and the loads [5]-[7]. Normally, both primary and secondary coils of the transformer are connected in Y-windings in distribution systems.

Conventionally, a cascaded controller including an outer voltage control and inner current control loops has been suggested [8]. However, its control dynamic response is slow since the voltage control loop has the limited bandwidth [5]. Also, when there are unbalanced voltage sags, the source voltage contains the negative sequence and zero-sequence components and hence, the d-q components of the source voltage can not be DC signals. Normally, a typical PI (proportional integral) controller does not work well for controlling the AC signals. Thus, a resonant control scheme has been employed to regulate the unified power quality conditioner, to compensate the load voltages under unbalanced and distorted conditions of source voltage and load [9]. Another issue considered for controlling the UPS (uninterruptible power supply) or DVR is the nonlinearity of the UPS or DVR [10], [11]. Thus, the nonlinear control gives better performance than the control techniques based on the PI control.

In the paper, a control method based on a sliding mode (SM) has been applied to improve the operation of the three-phase four-wire (3P4W) DVR system under grid fault conditions and nonlinear loads. First, the nonlinear model of the system including LC filter is obtained in the dq0 synchronous reference frame. Then, the controller design depending on the sliding mode control is performed, in which the load voltages are kept almost sinusoidal. The simulation results show the validity of the proposed control method.

## II. OVERVIEW OF DVR SYSTEM

### A. System modeling

The three-phase DVR circuit in Figure 1 can be represented in synchronous dq0 reference frame. Due to conditions of grid voltage sags and nonlinear loads, the dq0-axis components are taken into account as [11], [12]:

$$\dot{i}_{fdq} = \frac{1}{L_f} v_{dq} - \frac{1}{L_f} v_{cdq} - j\omega i_{fdq} \quad (1)$$

$$\dot{i}_{f0} = \frac{1}{(L_f + 3L_n)} v_0 - \frac{1}{(L_f + 3L_n)} v_{c0} \quad (2)$$

Tác giả liên hệ: Nguyen Trong Huan

Email: [huannt@ptithcm.edu.vn](mailto:huannt@ptithcm.edu.vn)

Đến tòa soạn: 9/2020; chỉnh sửa: 11/2020; chấp nhận đăng: 12/2020.

$$\dot{v}_{cdq} = \frac{1}{C_f} i_{dq} - \frac{1}{C_f} i_{fdq} - j\omega v_{cdq} \quad (3)$$

$$\dot{v}_{c0} = \frac{1}{C_f} i_{f0} - \frac{1}{C_f} i_0 \quad (4)$$

where  $L_f$ ,  $L_n$ , and  $C_f$  are the filter inductance, the neutral filter inductance, and the filter capacitance, respectively;  $v_{cdq0}$  are the  $dq0$ -axis capacitor voltages;  $v_{dq0}$  are the  $dq0$ -axis inverter terminal voltages;  $i_{dq0}$  are the  $dq0$ -axis output currents of the DVR;  $i_{fdq0}$  are the  $dq0$ -axis output currents;  $\omega$  is the source angular frequency.

From (1) to (4), a state-space modeling of the system is derived as follows:

$$\begin{bmatrix} \dot{i}_{fd} \\ \dot{i}_{fq} \\ \dot{i}_{f0} \\ \dot{v}_{cd} \\ \dot{v}_{cq} \\ \dot{v}_{c0} \end{bmatrix} = \begin{bmatrix} 0 & \omega & 0 & -1/L_f & 0 & 0 \\ -\omega & 0 & 0 & 0 & -1/L_f & 0 \\ 0 & 0 & 0 & 0 & 0 & -\frac{1}{L_f + 3L_n} \\ 1/C_f & 0 & 0 & 0 & \omega & 0 \\ 0 & 1/C_f & 0 & -\omega & 0 & 0 \\ 0 & 0 & 1/C_f & 0 & 0 & 0 \end{bmatrix} \begin{bmatrix} i_{fd} \\ i_{fq} \\ i_{f0} \\ v_{cd} \\ v_{cq} \\ v_{c0} \end{bmatrix} \quad (5)$$

$$+ \begin{bmatrix} 1/L_f & 0 & 0 \\ 0 & 1/L_f & 0 \\ 0 & 0 & \frac{1}{L_f + 3L_n} \\ 0 & 0 & 0 \\ 0 & 0 & 0 \\ 0 & 0 & 0 \end{bmatrix} \begin{bmatrix} v_d \\ v_q \\ v_0 \end{bmatrix} + \begin{bmatrix} 0 \\ 0 \\ 0 \\ i_d/C_f \\ i_q/C_f \\ i_0/C_f \end{bmatrix}$$

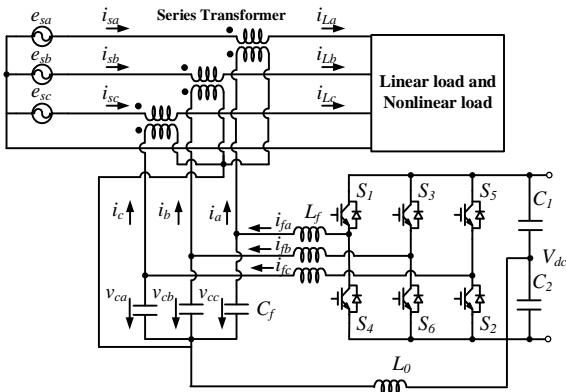


Figure 1. Circuit configuration of three-phase four-wire DVR.

### B. Generation of voltage references

In this research, the strategy of in-phase compensation is considered, in which the amplitude of the load voltage is exactly kept the same as before the sag, while the phase of the load voltage is similar to that of the source voltage after the sag. As shown in Figure 1, the load voltage is expressed as:

$$v_{L,abc} = e_{s,abc} - v_{dvr,abc} \quad (6)$$

where  $v_{L,abc}$  is the load voltage,  $e_{s,abc}$  is the d-q axis capacitor voltage, and  $v_{dvr,abc}$  is the voltage injected by the DVR.

The control of the DVR is performed in the synchronous reference frame, in which the phase angle of the source voltage is used for transforming the DVR output voltages and load voltages. To keep the load voltage constant, the

voltage references ( $v_{dvr,dq0}^*$ ) for the DVR system in the synchronous reference frame are calculated as:

$$v_{dvr,dq0}^* = e_{s,dq0} - v_{L,dq0}^* \quad (7)$$

where  $e_{s,dq0}$  is the  $dq0$ -axis components of the source voltage, and  $v_{L,dq0}^*$  is the  $dq0$ -axis components of the load voltage references, in which both  $v_{L,d}^*$  and  $v_{L,0}^*$  are also set to be zero and  $v_{L,q}^*$  is set to be magnitude of the load voltage at the rating ( $v_{L,mag}$ ).

### III. PROPOSED CONTROL STRATEGY USING SLIDING MODE CONTROL

A multi-input multi-output (MIMO) nonlinear approach is proposed for the purpose of eliminating the nonlinearity in the modeled system [10]. Consider a MIMO system as follows:

$$\dot{x} = f(x) + g \cdot u \quad (8)$$

$$y = h(x) \quad (9)$$

where  $x$  is state vector,  $u$  is control input,  $y$  is output,  $f$  and  $g$  are smooth vector fields,  $h$  is smooth scalar function.

The dynamic model of the inverter in (5) is expressed in (8) and (9) as:

$$x = [i_{fd} \quad i_{fq} \quad i_{f0} \quad v_{cd} \quad v_{cq} \quad v_{c0}]^T;$$

$$u = [v_d \quad v_q \quad v_0]^T;$$

$$y = [v_{cd} \quad v_{cq} \quad v_{c0}]^T$$

To generate an explicit relationship between the outputs  $y_{i=1,2,3}$  and the inputs  $u_{i=1,2,3}$ , each output is differentiated until a control input appears.

$$\begin{bmatrix} \ddot{y}_1 \\ \ddot{y}_2 \\ \ddot{y}_3 \end{bmatrix} = A(x) + E(x) \begin{bmatrix} u_1 \\ u_2 \\ u_3 \end{bmatrix} \quad (10)$$

Then, the control law is given as:

$$\begin{bmatrix} v_d^* \\ v_q^* \\ v_0^* \end{bmatrix} = \begin{bmatrix} u_1 \\ u_2 \\ u_3 \end{bmatrix} = E^{-1}(x) \left[ -A(x) + \begin{bmatrix} v_1 \\ v_2 \\ v_3 \end{bmatrix} \right] \quad (11)$$

where

$$A(x) = \begin{bmatrix} \frac{2}{C_f} \omega i_{fq} - \left( \frac{1}{L_f C_f} + \omega^2 \right) v_{cd} - \frac{1}{C_f} \dot{i}_d - \frac{1}{C_f} \omega i_q \\ -\frac{2}{C_f} \omega i_{fd} - \left( \frac{1}{L_f C_f} + \omega^2 \right) v_{cq} - \frac{1}{C_f} \dot{i}_q + \frac{1}{C_f} \omega i_d \\ -\frac{1}{(L_f + 3L_n) C_f} v_{c0} - \frac{1}{C_f} \dot{i}_{f0} \end{bmatrix};$$

$$E(x) = \begin{bmatrix} \frac{1}{L_f C_f} & 0 & 0 \\ 0 & \frac{1}{L_f C_f} & 0 \\ 0 & 0 & \frac{1}{(L_f + 3L_n) C_f} \end{bmatrix}$$

and  $v_1$ ,  $v_2$  and  $v_3$  are new control inputs.

The sliding surfaces with the errors of the indirect component voltages are expressed as [11]:

$$\begin{aligned} s_1 &= \ddot{e}_1 + k_{11}\dot{e}_1 + k_{12} \int e_1 dt \\ s_2 &= \ddot{e}_2 + k_{21}\dot{e}_2 + k_{22} \int e_2 dt \\ s_3 &= \ddot{e}_3 + k_{31}\dot{e}_3 + k_{32} \int e_3 dt \end{aligned} \quad (12)$$

where  $e_1 = y_1^* - y_1$ ,  $e_2 = y_2^* - y_2$  and  $e_3 = y_3^* - y_3$ ;  $y_1^*$ ,  $y_2^*$  and  $y_3^*$  are the reference values of the  $y_1$ ,  $y_2$  and  $y_3$ , respectively, and  $k_{11}$ ,  $k_{12}$ ,  $k_{21}$ ,  $k_{22}$ ,  $k_{31}$  and  $k_{32}$  are the positive constant gains.

By using a sliding mode control theory, the equivalent control input can be derived as the continuous control input that  $\dot{s}_1 = \dot{s}_2 = \dot{s}_3 = 0$  yields.

$$\begin{aligned} u_{1eq} &= L_f C_f \left[ v_1 + \frac{2}{C_f} \omega i_{fd} + \left( \frac{1}{L_f C_f} + \omega^2 \right) v_{cd} + \frac{1}{C_f} i_d + \frac{1}{C_f} \omega i_q \right] \\ u_{2eq} &= L_f C_f \left[ v_2 + \frac{2}{C_f} \omega i_{fd} + \left( \frac{1}{L_f C_f} + \omega^2 \right) v_{cq} + \frac{1}{C_f} i_q - \frac{1}{C_f} \omega i_d \right] \\ u_{3eq} &= L_f C_f \left[ v_3 + \frac{1}{(L_f + 3L_n) C_f} v_{e0} + \frac{1}{C_f} i_{f0} \right] \end{aligned} \quad (13)$$

To drive the state variables to the sliding surface  $s_1 = s_2 = s_3 = 0$ , in the case of  $s_1 \neq 0$ ,  $s_2 \neq 0$ ,  $s_3 \neq 0$ , the control laws are defined as:

$$\begin{aligned} u_1 &= u_{1eq} + \gamma_1 \text{sign}(s_1) \\ u_2 &= u_{2eq} + \gamma_2 \text{sign}(s_2) \\ u_3 &= u_{3eq} + \gamma_3 \text{sign}(s_3) \end{aligned} \quad (14)$$

where  $\gamma_1 > 0$ ,  $\gamma_2 > 0$ ,  $\gamma_3 > 0$ .

The reaching law can be derived by substituting (14) into (12), which gives

$$\dot{s}_1 = -\gamma_1 \text{sign}(s_1); \quad \dot{s}_2 = -\gamma_2 \text{sign}(s_2) \quad (15)$$

In order to determine the stability and robustness, Lyapunov's functions which are presented in [12], are defined as follows:

$$\begin{cases} V_1 = \frac{1}{2} s_1^2 \\ V_2 = \frac{1}{2} s_2^2 \end{cases} \quad (16)$$

By taking time derivative of  $V_1$  and  $V_2$ , to prove stability, the following condition must be satisfied

$$\begin{cases} \dot{V}_1 = s_1 \dot{s}_1 < 0 \\ \dot{V}_2 = s_2 \dot{s}_2 < 0 \end{cases} \quad (17)$$

Figure 2 shows the block diagram of the sliding mode controller, in which the dq0-axis voltage references are obtained from (7).

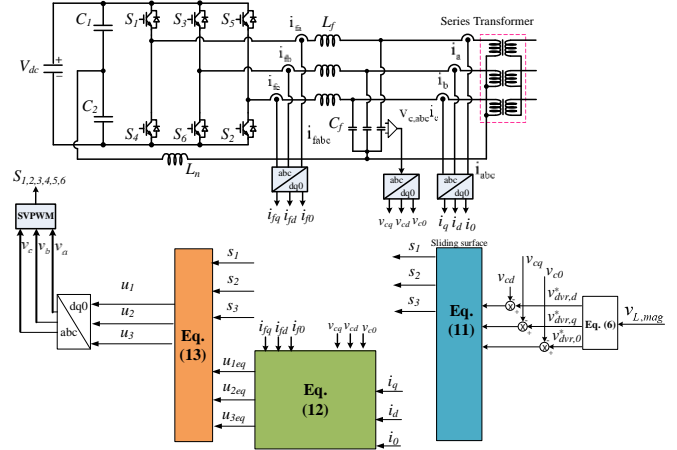


Figure 2. Block diagram of the proposed controller.

The system output response to its command is evaluated by the resonant peak and bandwidth values in the Bode plot. In order to compare with conventional method, the PI control technique is also proposed as shown in Figure 3. Then, the closed-loop transfer function of the cascade PI controllers is derived as:

$$\frac{v_{dvr}}{v_{dvr}^*} = \frac{k_p k_p s^2 + (k_p k_i s + k_i k_p) s + k_i k_i}{L_f C_f s^4 + k_p C_f s^3 + (k_i C_f + k_p k_p) s^2 + (k_p k_i s + k_i k_p) s + k_i k_i} \quad (18)$$

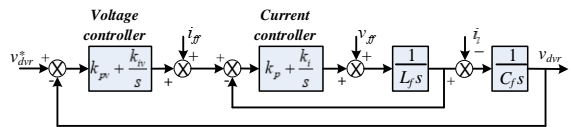


Figure 3. Control block diagram of DVR using PI control for voltage and current controllers.

The Bode plot of the closed-loop transfer function of two controllers is analyzed in Figure 4. At the low-frequency range, the two controllers have a unity gain and zero phase delay. However, The sliding mode control has a lower resonant peak and a wider bandwidth which results in a lower overshoot and a faster settling time at the stepwise load change. Thus, the performance of the sliding mode control is better than that of the PI control.

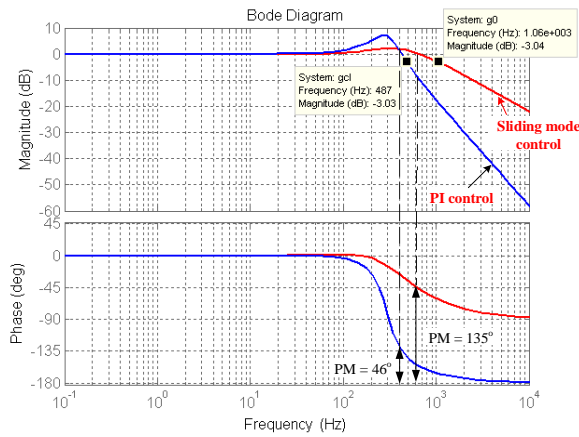


Figure 4. Bode plot of the closed-loop sliding mode control and PI voltage controller.

IV. SIMULATION RESULTS

PSIM simulations have been carried out for the unbalanced and nonlinear loads to verify the feasibility of the proposed method. A DC-link voltage at the input of inverter is 400[V], the switching frequency of inverter is 10[kHz]. The grid voltage is 180V<sub>rms</sub>/60Hz. The parameters of loads and controllers are shown in the Table 1 and Table 2, respectively.

Table 1. Parameters of loads

Type of load	Parameters
Nonlinear load	L = 3 [mH], C = 1000 [μF], R = 30 [Ω]

Table 2. Parameters of controllers

Controller Type		Gains of controller
		Nonlinear load
PI control	Current controller	k <sub>p</sub> = 17.5 k <sub>i</sub> = 13100
	Voltage controller	k <sub>pV</sub> = 0.31 k <sub>iV</sub> = 892
Proposed control		k <sub>11</sub> =k <sub>21</sub> = k <sub>31</sub> = 4.4 x 10 <sup>3</sup> , k <sub>12</sub> = k <sub>22</sub> =k <sub>32</sub> = 8.4 x 10 <sup>6</sup>

The simulation results for the PI control and proposed control method under the conditions of grid voltage sags and linear loads are shown in Figures 4 and 5, respectively. The grid fault is assumed to be unbalanced voltage sags, in which voltages of phases a, b, and c drop to 50%, 75% and 50%, respectively for 40 [ms].

When the DVR is activated, the DVR output voltages are injected and load voltages should be kept unchanged. Moreover, the load voltages after the sag must be sinusoidal and balanced, like those before pre-sag.

Figure 4 shown the performance of the DVR with the conventional PI control under the conditions of grid voltage sags and linear loads. The DVR output voltage is shown in Figure 4(b) and the load voltage is sinusoidal but still has some ripple, as shown in Figure 4(c). It is illustrated from Figure 4 (d) to (f) that, the actual values of the dq0 axis DVR voltage components track their references. The load currents are illustrated in Figure 4(g).

Under the same simulation conditions of grid voltage sags and linear loads, as shown in Figure 4(a), the control performance of the DVR with the proposed method is shown in Figure 5. Figure 5(c) shows the load voltages, which are kept at nominal values even though the grid voltages drop, as shown in Figure 5(a). The output voltages of the DVR to compensate for the voltage sags are shown in Figure 5(b). It is illustrated in Figure 5(d)–(f) that, the actual values of the dq0 axis DVR voltage components with the proposed strategy track their references well, which are much better than those of the conventional ones, especially with the method based on the classical PI controllers as shown in Figure 4 (d) –(f), respectively. In comparison with the PI controller, the total harmonic distortion (THD) analysis for load voltage is shown in Table 3, in which the proposed controller gives better results with lower THD.

Table 3. Total harmonic distortion (THD) analysis of three-phase load voltages using PI and proposed controllers.

Controller Type	THD (%)					
	Linear load			Nonlinear load		
	Phase A	Phase B	Phase C	Phase A	Phase B	Phase A
PI control	2.53	2.14	2.69	3.30	2.48	2.80
Proposed control	1.96	1.83	2.34	2.13	1.96	2.39

The performance of the DVR with the conventional PI control under the conditions of grid voltage sags and nonlinear loads is shown in Figure 6, in which voltages of phases a, b, and c also drop to 50%, 75% and 50%, respectively for 40 [ms]. The DVR output voltage is shown in Figure 6(b). The waveform of the load voltage is distorted due to the influence of the nonlinear load Figure 6(c). This shows that the conventional control method do not respond well. The actual values of the dq0 axis DVR voltage components are shown from Figure 6(d) to (f), respectively. The load currents are illustrated in Figure 6(g). On the contrary, for the proposed control method, the control performance of the DVR is shown in Figure 7. As can be seen from Figure 7(d) to (f) that, the actual values of the dq0 axis DVR voltage components with the proposed strategy follow their references well, which are much better than those of the conventional ones, as shown in Figure 6 (d) –(f), respectively. Figure 7(c) shows the load voltages, which are kept at nominal values even though the grid voltages drop, and no distortion due to the influence of nonlinear load as shown in Figure 7(a). The output voltages of the DVR to compensate for the voltage sags are shown in Figure 7(b).

Based on THD analysis results in Table 3 for the case of using nonlinear loads, it can be seen that THD of the proposed controller has better results than the PI controller. Finally, with the same condition, the DVR control in the proposed method works satisfactorily, since the d-q component voltages of the DVR are well regulated.

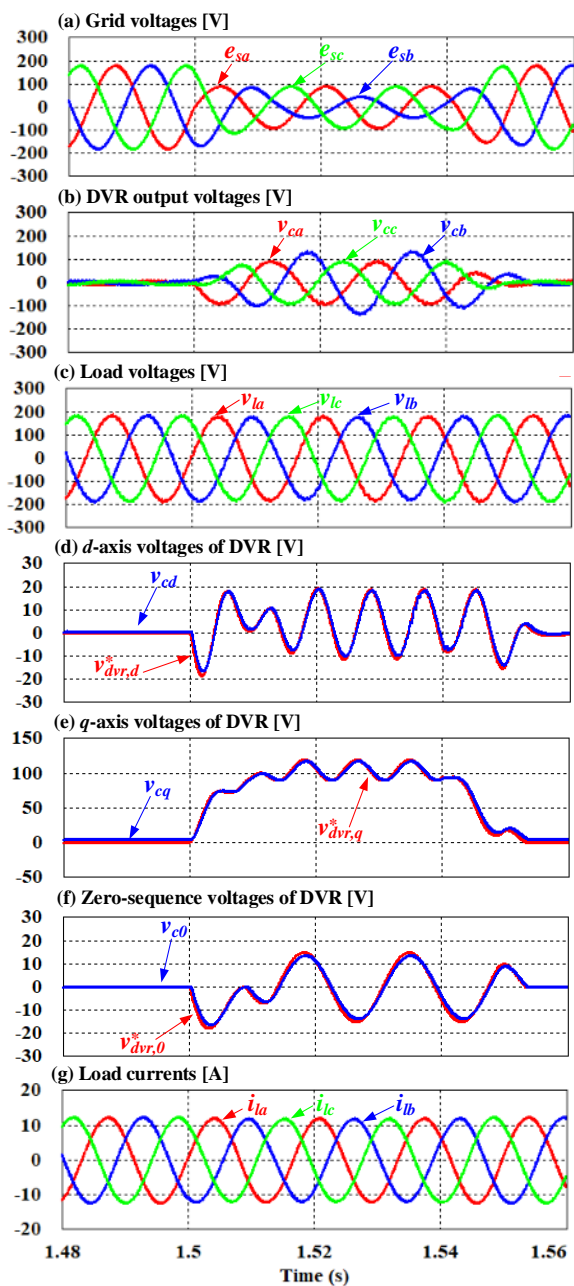


Figure 4. Dynamic response of PI control method under the conditions of grid voltage sags and linear loads. (a) Grid voltages. (b) DVR output voltages. (c) Load voltages. (d)  $d$ -axis voltages of DVR. (e)  $q$ -axis voltages of DVR. (f) Zero-sequence voltages of DVR. (g) Load currents.

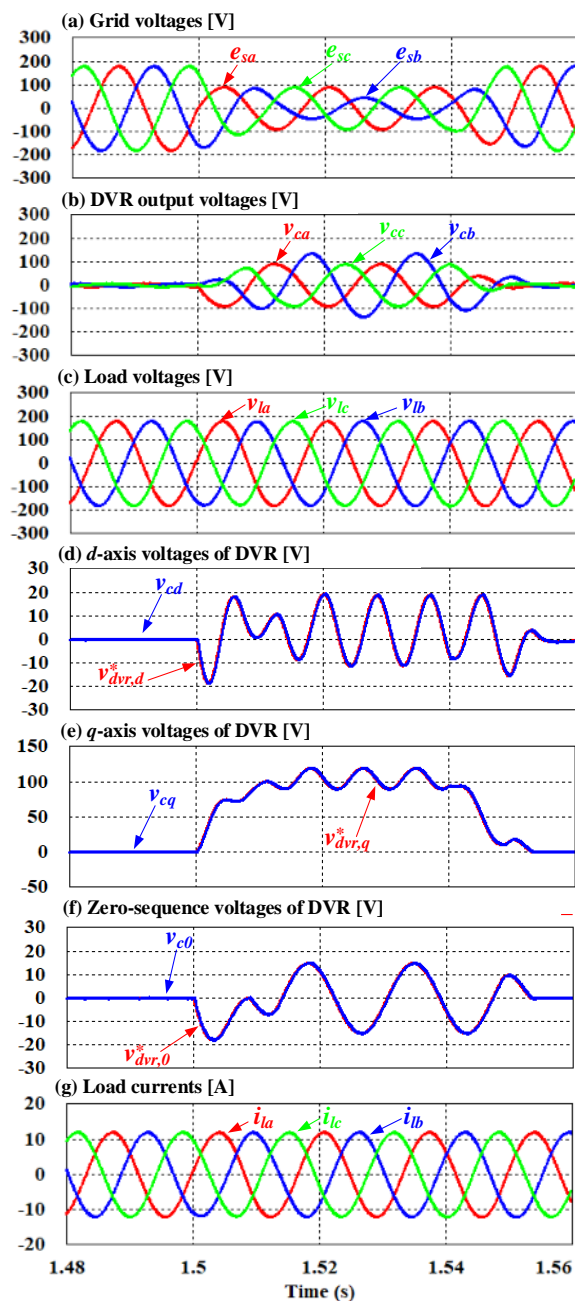


Figure 5. Dynamic response of proposed control method under the conditions of grid voltage sags and linear loads. (a) Grid voltages. (b) DVR output voltages. (c) Load voltages. (d)  $d$ -axis voltages of DVR. (e)  $q$ -axis voltages of DVR. (f) Zero-sequence voltages of DVR. (g) Load currents.

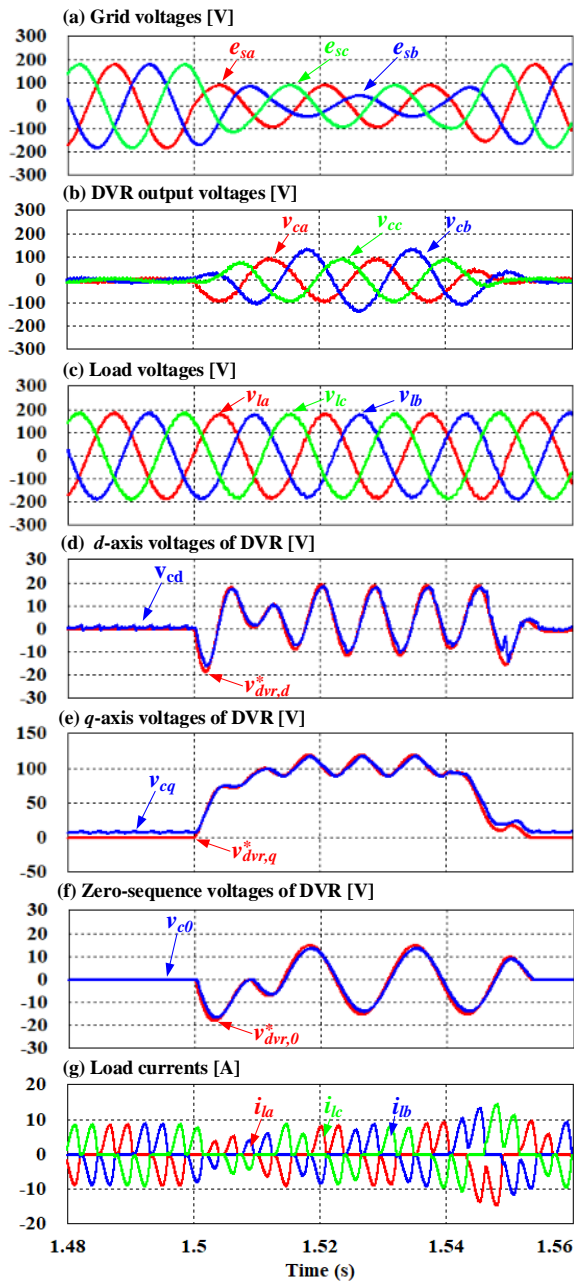


Figure 6. Dynamic response of PI control method under the conditions of grid voltage sags and nonlinear loads. (a) Grid voltages. (b) DVR output voltages. (c) Load voltages. (d)  $d$ -axis voltages of DVR. (e)  $q$ -axis voltages of DVR. (f) Zero-sequence voltages of DVR. (g) Load currents.

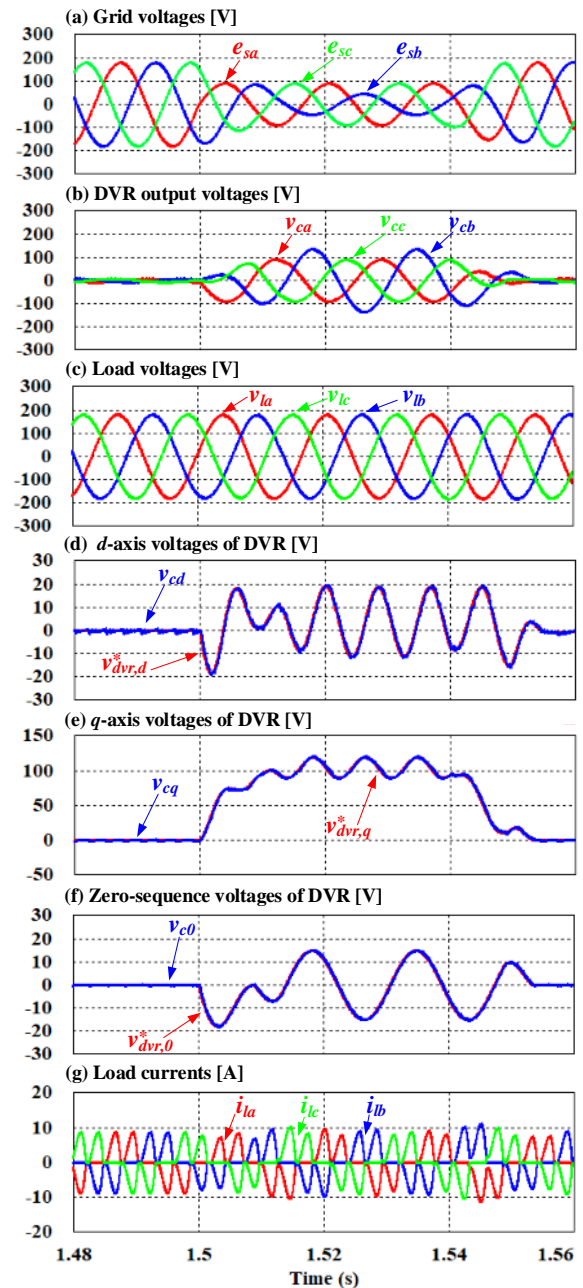


Figure 7. Dynamic response of proposed control method under the conditions of grid voltage sags and nonlinear loads. (a) Grid voltages. (b) DVR output voltages. (c) Load voltages. (d)  $d$ -axis voltages of DVR. (e)  $q$ -axis voltages of DVR. (f) Zero-sequence voltages of DVR. (g) Load currents.

## V. CONCLUSION

In this paper, an advanced control strategy for the DVR was proposed. The effectiveness of the proposed control strategy was verified through simulation tests, in which the load voltage is almost sinusoidal and in-phase with the supply voltage even under the conditions of grid voltage sags and linear or nonlinear loads. The feasibility of the proposed control is verified by simulation results, which show the better performance than conventional PI method. For the further work, the experiment must be implemented with using DSP F28379D to show effectiveness of the proposed control in the real system.

REFERENCES

- [1] Trinh Q. N., Lee H.-H., and Chun T. W., An enhanced harmonic voltage compensator for general loads in standalone distributed generation systems, *Journal of Power Electronics*, Vol. 13, No. 6, pp. 1070-1079, 2013.
- [2] Babaei E., Kangarlu M. F., and Sabahi M., Mitigation of voltage disturbances using dynamic voltage restorer based on direct converters, *IEEE Transactions on Power Electronics*, Vol. 25, No. 4, pp. 2676-2683, 2010.
- [3] Xu H., Ma X., and Sun D., Reactive current assignment and control for DFIG based wind turbines during grid voltage sag and swell conditions, *Journal of Power Electronics*, Vol. 15, No. 1, pp. 235-245, 2015.
- [4] Khadkikar V. and Chandra A., UPQC-S: a novel concept of simultaneous voltage sag/swell and load reactive power compensations utilizing series inverter of UPQC, *IEEE Transactions on Power Electronics*, Vol. 26, No. 9, pp. 2414-2425, 2011.
- [5] Kim H. and Sul S.-K., Compensation voltage control in dynamic voltage restorers by use of feed forward and state feedback scheme, *IEEE Transactions on Power Electronics*, Vol. 20, No. 5, pp. 1169-1177, 2005.
- [6] Jimichi T., Fujita H., and Akagi H., Design and experimentation of a dynamic voltage restorer capable of significantly reducing an energy-storage element, *IEEE Transactions on Industry Applications*, Vol. 44, No. 3, pp. 817-825, 2008.
- [7] Meyer C., De Doncker R. W., Li Y. W., and Blaabjerg F., Optimized control strategy for a medium-voltage DVR theoretical investigations and experimental results, *IEEE Transactions on Power Electronics*, Vol. 23, No. 6, pp. 2746-2754, 2008.
- [8] Lee S., Chae Y., Cho J., Choe G., Mok H., and Jang D., A new control strategy for instantaneous voltage compensator using 3-phase PWM inverter, in Proc. IEEE PESC'98, pp. 248-254, 1998.
- [9] Trinh Q.-N. and Lee H.-H., Improvement of unified power quality conditioner performance with enhanced resonant control strategy, *IET Generation Transmission Distribution*, Vol. 8, No.12, pp. 2114-2123, 2014.
- [10] Kim D.-E. and Lee D.-C., Feedback linearization control of three-phase UPS inverter system, *IEEE Transactions on Industrial Electronics*, Vol. 57, No. 3, pp. 963-968, 2010.
- [11] Khalifa Al H., Thanh Hai N., Naji Al S., "An improved control strategy of 3P4W DVR systems under unbalanced and distorted voltage conditions", *Electrical Power and Energy Systems*, Vol. 98, pp. 233-242, 2018.
- [12] Van T. L., Nguyen T. H., Ho N. M., Doan X. N., and Nguyen T. H., "Voltage Compensation Scheme for DFIG Wind Turbine System to Enhance Low Voltage Ride-Through Capability", *10th International Conference on Power Electronics (ECCE Asia)*, pp.1334-1338, 2019.
- [13] Slotine J.-J. E. and Li W., *Applied Nonlinear Control*. Englewood Cliffs, NJ: Prentice-Hall, pp. 207-271, 1991.

**CHIẾN LƯỢC ĐIỀU KHIỂN BỘ LƯU TRỮ ĐIỆN ÁP ĐỘNG TRONG ĐIỀU KIỆN SỤT ĐIỆN ÁP LƯỚI VÀ TẢI PHI TUYẾN**

**Tóm tắt** - Trong bài báo này, mô hình điều khiển phi tuyến cho bộ lưu trữ điện áp động (DVR) được đề xuất để giảm nhiễu điện áp cho tải dưới điều kiện sụt điện áp lưới và tải phi tuyến. Đầu tiên, mô hình phi tuyến của hệ thống bao gồm bộ lọc LC được biểu diễn trong hệ quy chiếu đồng bộ dq0. Sau đó, quá trình thiết kế bộ điều khiển được thực hiện bằng cách sử dụng bộ điều khiển trượt, trong đó điện áp tải được duy trì gần như hình sin bằng cách điều khiển các thành phần trục dq0 của điện áp ngõ ra bộ DVR. Với mô hình này, chất lượng điện năng được cải thiện đáng kể so với bộ điều khiển tích phân tỷ lệ (PI) thông thường trong

điều kiện sụt điện áp lưới và tải phi tuyến. Các nghiên cứu mô phỏng được thực hiện để kiểm tra hiệu quả của phương pháp được đề xuất.

**Từ khóa** - Bộ lưu trữ điện áp động, tải phi tuyến, điều khiển trượt, sụt áp.



**Nguyen Trong Huan** was born in VietNam in 1986. He received his undergraduate degree in 2010, major in Electrical and Electronics Technology from University of Technical Education of Ho Chi Minh City. In 2014, he received the Master of Telecommunication Engineering

Degree from Posts and Telecommunications Institute of Technology, Ho Chi Minh City Campus. He is working at Department of Electrical and Electronic Engineering, Posts and Telecommunications Institute of Technology, Ho Chi Minh City Campus, VietNam.



**Ho Nhut Minh** was born in Vietnam in 1987. He received his undergraduate degree in 2010, major in Electronics & Telecommunications Engineering from University of Technical Education of Ho Chi Minh City. In 2014, he received the Master of

Telecommunication Engineering Degree from Posts and Telecommunications Institute of Technology, Ho Chi Minh City Campus. He is working at Department of Electrical and Electronic Engineering, Posts and Telecommunications Institute of Technology, Ho Chi Minh City Campus, VietNam.



**Van Tan Luong** was born in Vietnam. He received the B.Sc. and M.Sc. degrees in electrical engineering from Ho Chi Minh City University of Technology, Ho Chi Minh city, Vietnam, in 2003 and 2005, respectively, and Ph.D. degree in electrical engineering from Yeungnam University,

Gyeongsan, South Korea in 2013. Currently, he is working at Department of Electrical and Electronics Engineering, Ho Chi Minh city University of Food Industry. His research interests include power converters, machine drives, wind power generation, power quality and power system.